YMTHE, Volume *28*

Supplemental Information

Targeted Delivery of CXCL9 and OX40L by Mesenchymal Stem Cells Elicits Potent Antitumor Immunity

Pan Yin, Liming Gui, Caihong Wang, Jingjing Yan, Min Liu, Lu Ji, You Wang, Bin Ma, and Wei-Qiang Gao

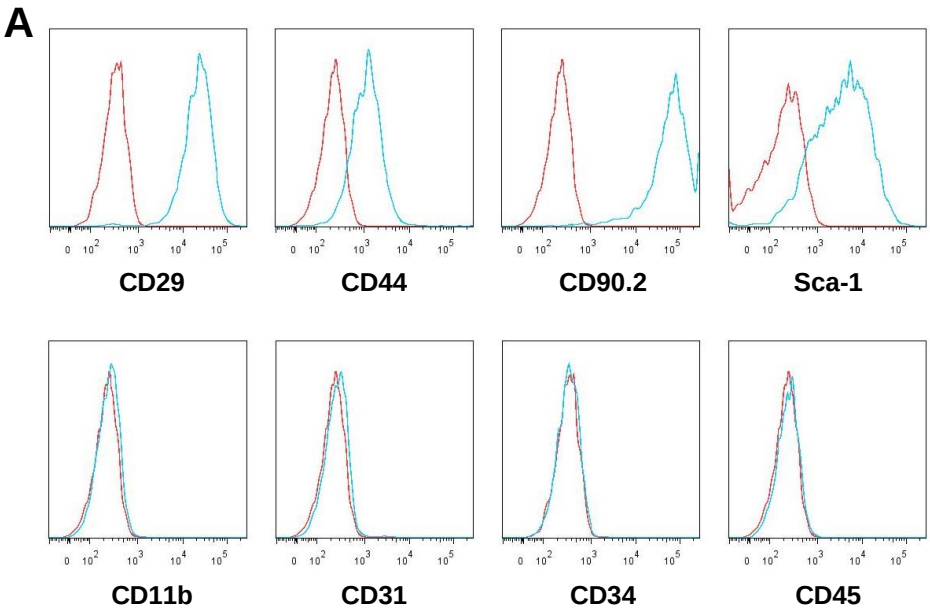

B

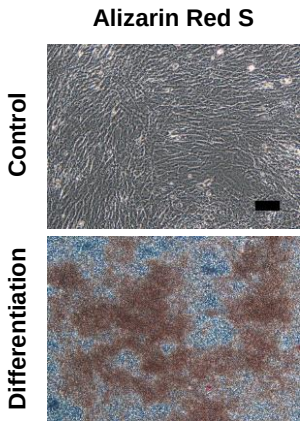

C

MSCs injected ($\times 10^6$)	Subcutaneous tumors formed / mice injected
0.5	0/5
1.5	0/5
5.0	0/5

Figure S1. AT-MSCs exhibit osteogenic differentiation ability but no tumorigenic potential.

(**A**) Characterization of AT-MSCs isolated from C57BL/6 mice by FACS. (**B**) The ability of mouse AT-MSCs to differentiate into osteocytes was determined by Alizarin Red S staining. Scale bar = 200 μm. (**C**) Different numbers of AT-MSCs isolated from BALB/c mice were injected subcutaneously to BALB/c mice and tumor formation was evaluated for 60 days.

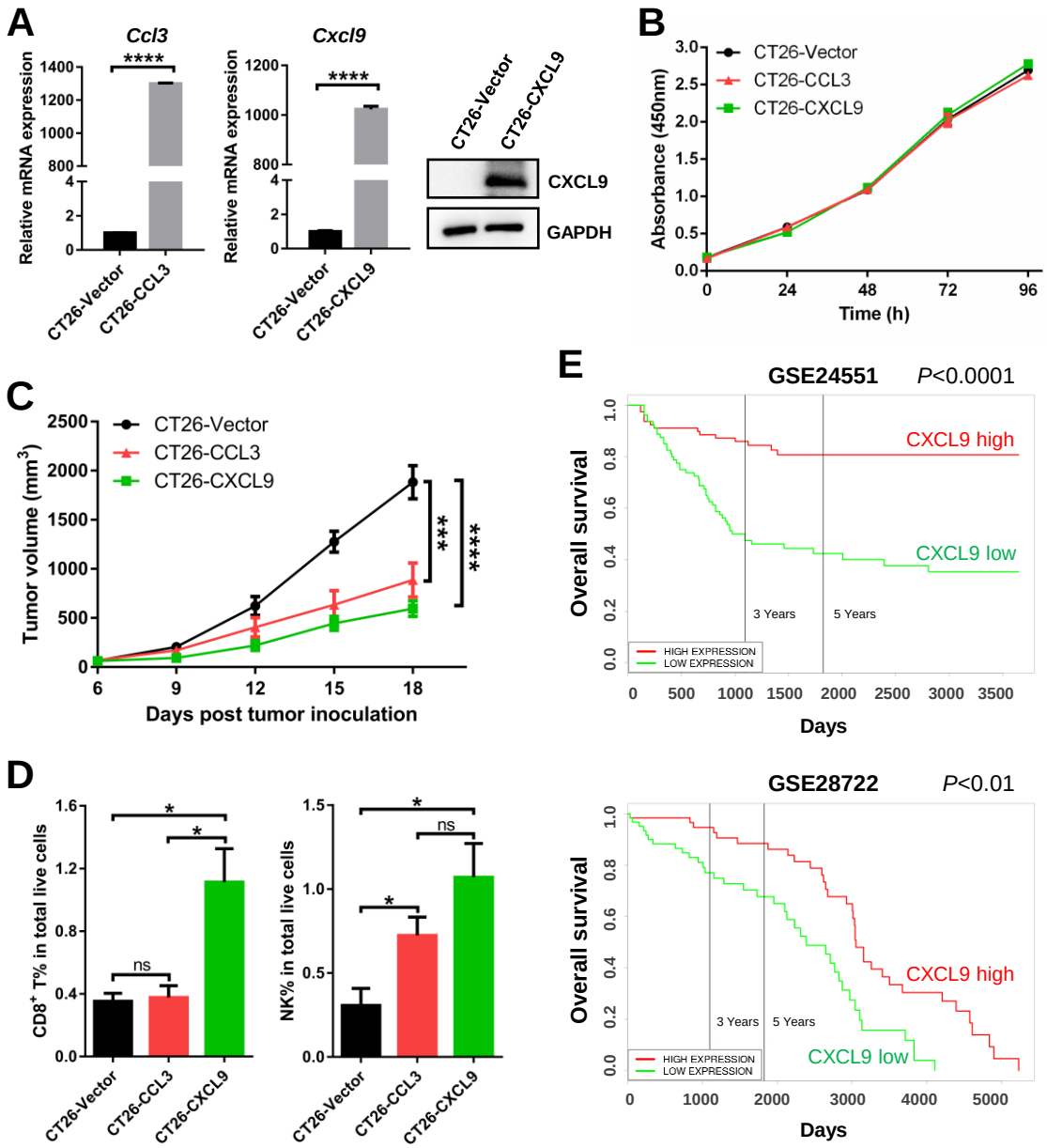

Figure S2. Tumoral expression of CXCL9 results in tumor regression.

(**A**) Detection of CCL3 and CXCL9 mRNA expression in CT26 by qPCR, and CXCL9 protein levels by Western blotting (n = 3). (**B**) Proliferation of CT26-Vector, CT26-CCL3 and CT26-CXCL9 cells was measured using CCK-8 assay (n = 3). (**C**) CT26-Vector, CT26-CCL3 or CT26-CXCL9 cells were injected subcutaneously into BALB/c mice, and the size of the tumor was monitored (n = 5 mice per group). (**D**) Percentages of the $CD8^+$ T and NK cells within total live cells were shown (n = 3). (**E**) Correlation of CXCL9 mRNA expression and survival rate in colorectal cancer patients (Datasets: GSE24551 and GSE28722). * $P < 0.05$, *** $P < 0.001$, **** $P < 0.0001$, ns = not significant.

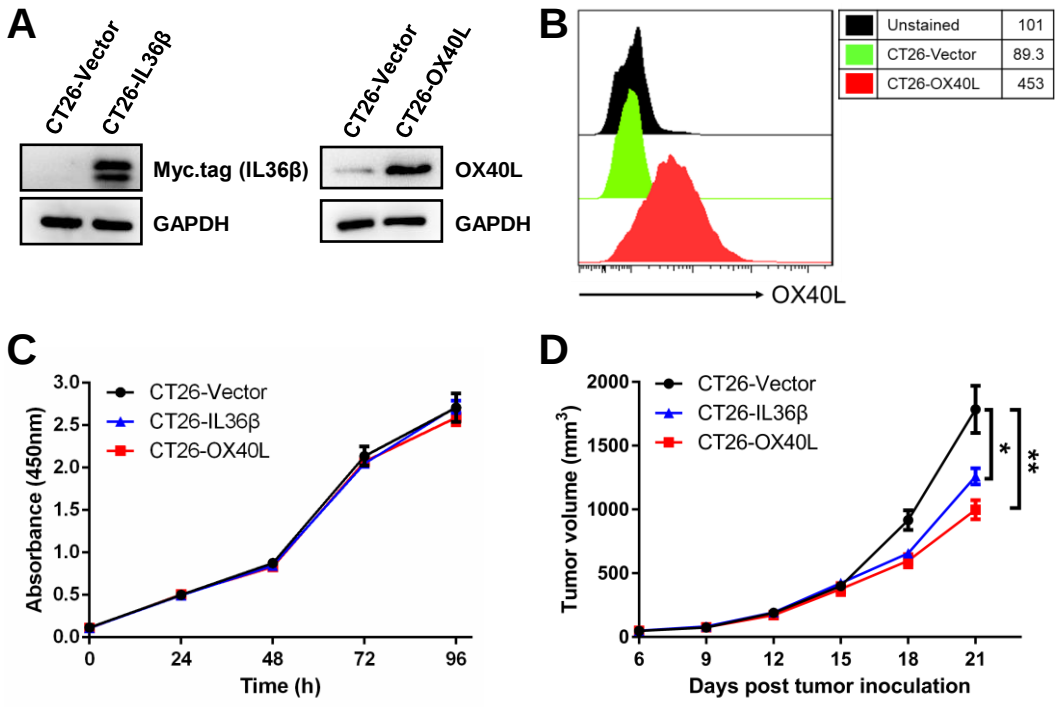

Figure S3. Tumoral expression of OX40L inhibits tumor growth.

(**A**) Expression of IL36β and OX40L proteins in CT26 was detected by Western blotting. (**B**) Expression of membrane-bound OX40L in CT26 was detected by FACS. (**C**) Proliferation of CT26-Vector, CT26-CCL3 and CT26-CXCL9 cells was evaluated using CCK-8 assay (n = 3). (**D**) CT26-vector or CT26-IL36β or CT26-OX40L cells were injected subcutaneously into BALB/c mice. The size of the tumor was recorded (n = 4 mice per group). * $P < 0.05$, ** $P < 0.01$.

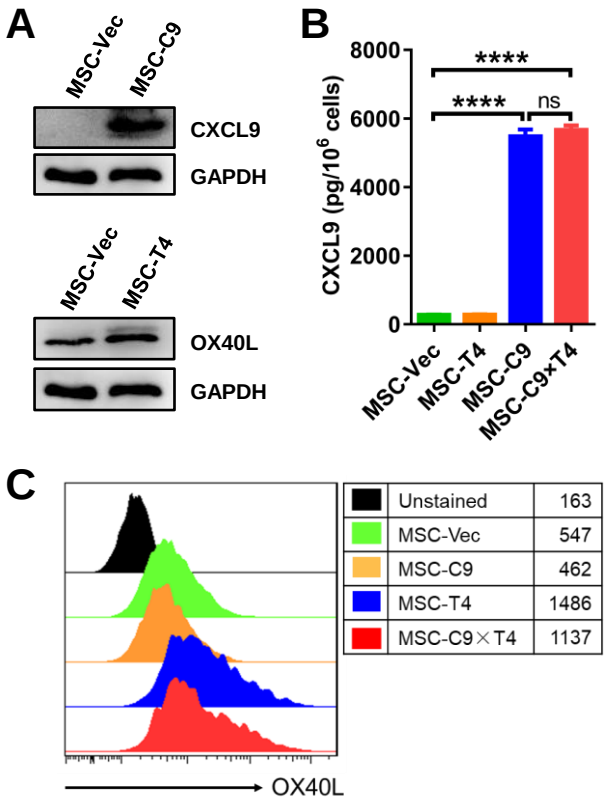

D

MSCs injected (5×10^6)	Subcutaneous tumors formed / mice injected
MSC-Vec	0/5
MSC-C9×T4	0/5

Figure S4. CXCL9 and OX40L are successfully overexpressed in AT-MSCs.

(**A**) Expression of CXCL9 and OX40L in AT-MSCs was detected by Western blotting. (**B**) Secretion of CXCL9 by transduced AT-MSCs was determined by ELISA (n = 4). (**C**) Expression OX40L on cell membranes was detected by flow cytometry. (**D**) AT-MSCs isolated from BALB/c mice were lentivirally transduced and injected subcutaneously to BALB/c mice and tumor formation was evaluated for 120 days. **** $P < 0.0001$, ns = not significant.

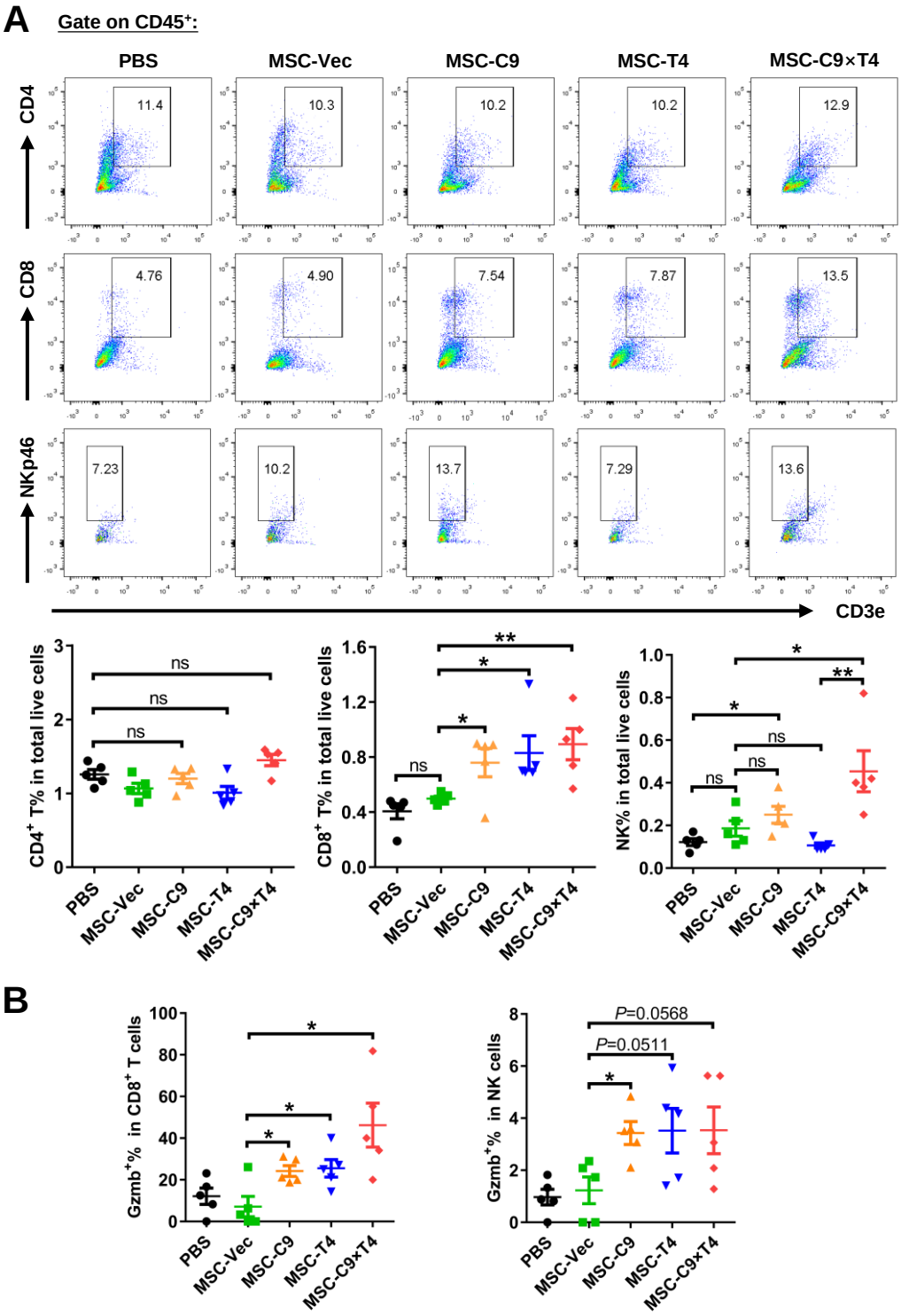

Figure S5. Delivery of CXCL9 and OX40L by AT-MSCs shapes MC38 tumor immune microenvironment.

(**A**) Tumor-infiltrating CD4$^+$ T, CD8$^+$ T, and NK cells were analyzed by FACS three days after the last injection of MSCs in MC38 tumor model (n = 5). (**B**) Expression of granzyme B (Gzmb) in CD8$^+$ T and NK cells was analyzed by flow cytometry (n = 5). * $P < 0.05$, ** $P < 0.01$, ns = not significant.

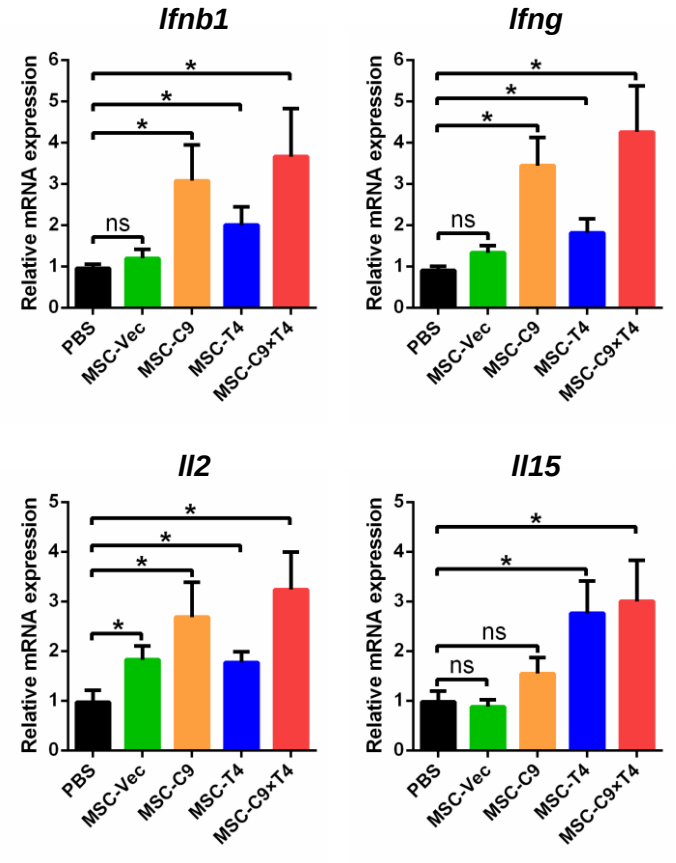

Figure S6. qPCR analysis of cytokine expression in MC38 tumors treated with engineered AT-MSCs.

Cytokine mRNA expression of MC38 tumors treated with MSC-Vec, MSC-C9, MSC-T4, MSC-C9×T4 or PBS was quantified using qPCR (n = 5). * $P < 0.05$, ns = not significant.

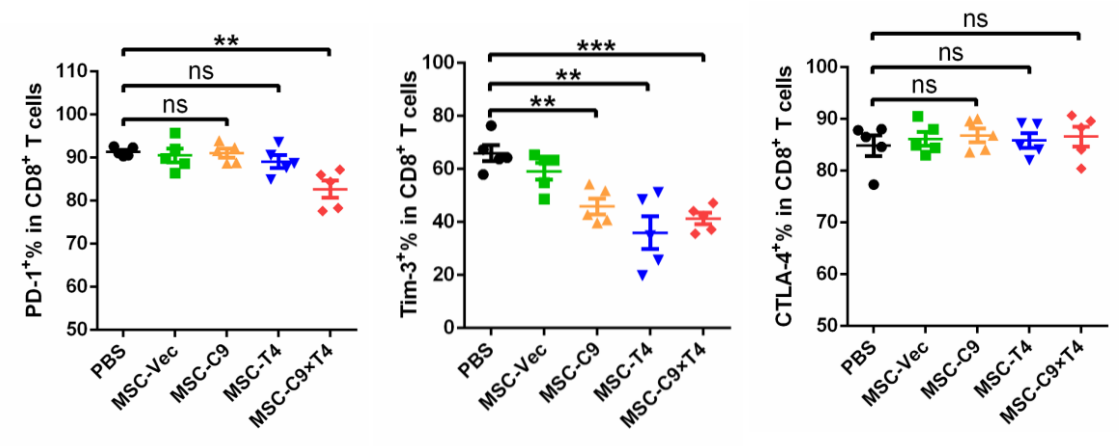

Figure S7. Expression of immune inhibitory molecules on tumor $CD8^+$ T cells upon MSC therapy.

Expression of PD-1, Tim-3 and CTLA-4 on $CD8^+$ T cells in MC38 tumors was analyzed by FACS (n = 5). ** $P < 0.01$, *** $P < 0.001$, ns = not significant.

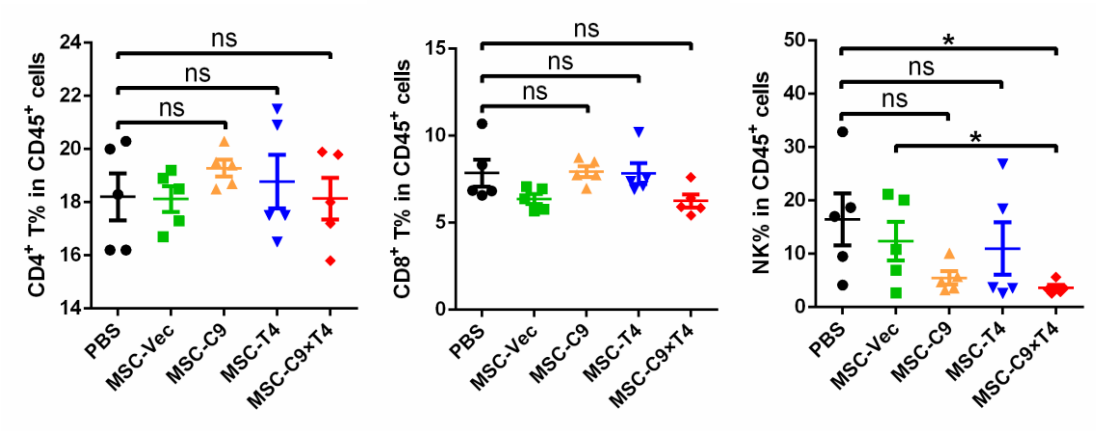

Figure S8. FACS analysis of splenic T and NK cells upon MSC therapy.

Splenic $CD4^+$ T, $CD8^+$ T, and NK cells were analyzed by FACS in MC38 mouse tumor models received MSC therapy (n = 5). * $P < 0.05$, ns = not significant.

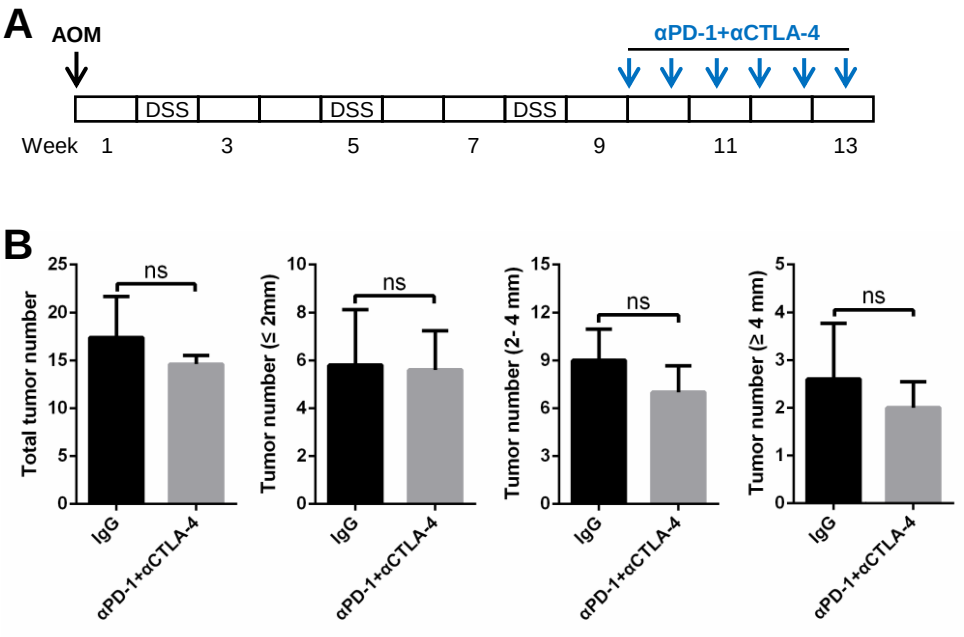

Figure S9. Checkpoint inhibitors do not impair colitis-associated cancer progression.

(**A**) Scheme of AOM/DSS administration and antibody treatment schedule. (**B**) Average number of tumors in different size ranges (n = 5 mice per group). ns = not significant.

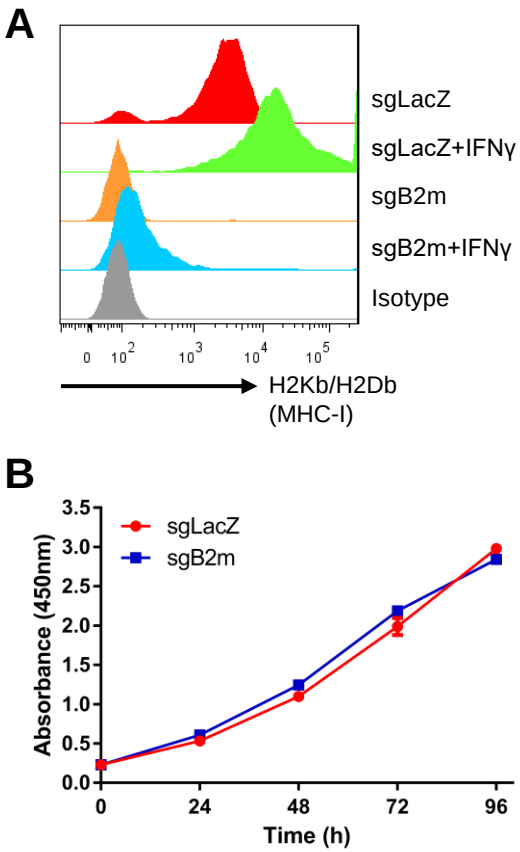

Figure S10. Absence of MHC-I on MC38 cells does not influence cell proliferation *in vitro*.

(**A**) FACS analysis of H2Kb/H2Db (MHC-I) on B2m-KO (sgB2m) and control (sgLacZ) MC38 cells *in vitro* with or without recombinant mouse IFN-γ stimulation. (**B**) Proliferation of MC38-sgB2m and MC38-sgLacZ cells *in vitro* was measured using CCK-8 assay (n = 4).

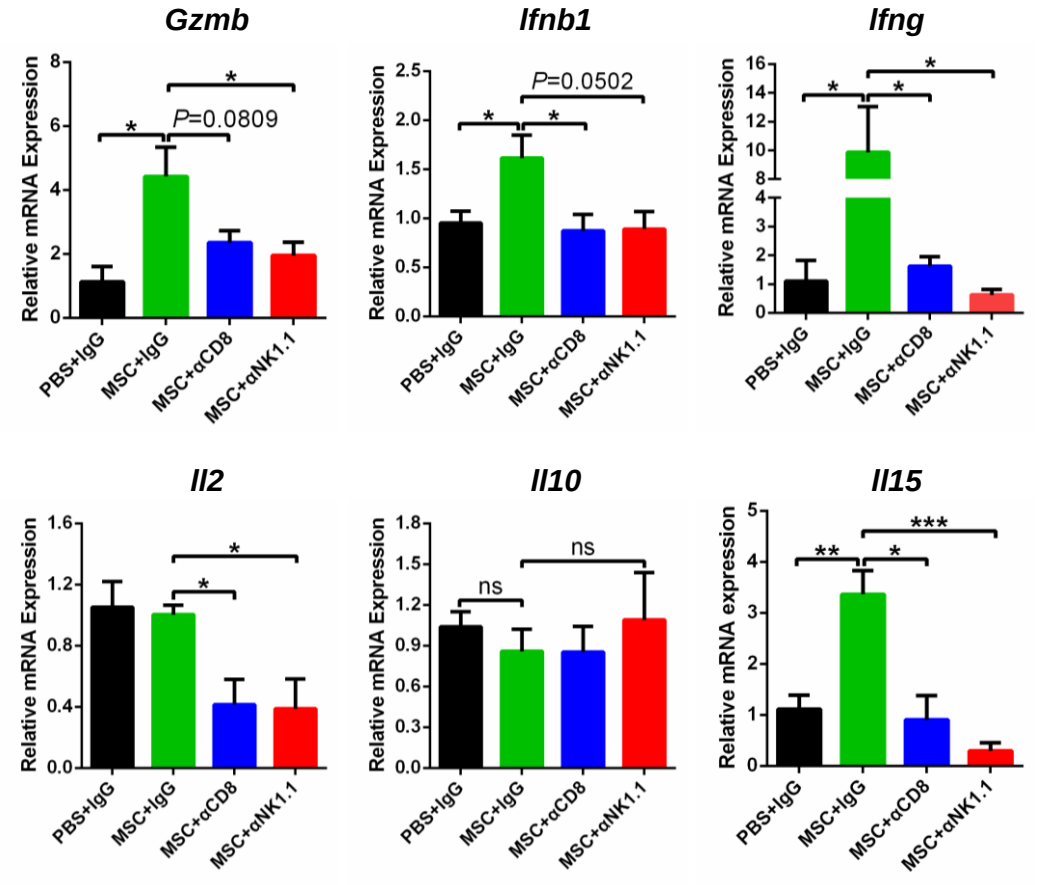

Figure S11. qPCR analysis of cytokine expression in MHC-I-deficient MC38 tumors treated with MSC-C9×T4.

Cytokine mRNA expression of MHC-I-deficient MC38 tumors treated with MSC-C9×T4 and αCD8/αNK1.1 depleting antibodies was quantified using qPCR (n = 4). * $P < 0.05$, ** $P < 0.01$, *** $P < 0.001$, ns = not significant.